Proceedings of DETC/CIE'02
2002 ASME Design Engineering Technical Conferences
September 29 - October 02, 2002, Montréal , Québec, Canada

DETC2002/MECH-34378

SOLVING THE BURMESTER PROBLEM USING KINEMATIC MAPPING

M.J.D. Hayes*
Carleton University
Deptartment of Mechanical &
Aerospace Engineering
1125 Colonel By Drive
Ottawa, Ontario,
Canada, K1S 5B6
Email: jhayes@mae.carleton.ca

P.J. Zsombor-Murray
McGill University
Dept. of Mechanical Engineering
Centre for Intelligent Machines
817 Sherbrooke St. W.
Montréal, Québec,
Canada, H3A 2K6
Email: paul@cim.mcgill.ca

ABSTRACT

Planar kinematic mapping is applied to the five-position Burmester problem for planar four-bar mechanism synthesis. The problem formulation takes the five distinct rigid body poses directly as inputs to generate five quadratic constraint equations. The five poses are on the fourth order curve of intersection of up to four hyperboloids of one sheet in the image space. Moreover, the five poses uniquely specify these two hyperboloids. So, given five positions of any reference point on the coupler and five corresponding orientations, we get the fixed revolute centres, the link lengths, crank angles, and the locations of the coupler attachment points by solving a system of five quadratics in five variables that always factor in such a way as to give two pairs of solutions for the five variables (when they exist).

1 Introduction

The determination of a planar four-bar mechanism that can guide a rigid-body through five finitely separated *poses* (position and orientation) is known as the *five-position Burmester problem*, see Burmester (1888). It may be stated as follows. Given five positions of a point on a moving rigid body and the corresponding five orientations of some line on that body, design a four-bar mechanism whose coupler crank pins are located on the moving body and is assemblable upon these five poses. The coupler must assume the five required poses, however sometimes not all five may lie in the same assembly branch.

The problem formulation engenders as many variables as equations so the synthesis is exact. However, most approaches to synthesizing a mechanism that can guide the rigid body exactly through the five positions are rooted in the Euclidean geometry of the plane in which the rigid body must move. From time to time this problem has been revisited (Chang, *et al*, 1991). Readers are refered to this document which contains a recent solution method and a quite adequate and relevant bibliography. More recently, classical finite position synthesis has been reviewed by McCarthy (2000).

We propose a solution obtained in a three-dimensional projective image space of the rigid body motion. An algebraic approach to this exact problem based on quaternions is to be found in Murray and McCarthy (1996). Instead, we use planar kinematic mapping. The planar kinematic mapping was introduced independently by Blaschke and Grünwald in 1911 (Blaschke, 1911; Grünwald, 1911). But, their writings are difficult. In North America Roth, De Sa, Ravani (De Sa and Roth, 1981; Ravani and Roth, 1983), as well as others, have made contributions. However, we choose to build upon interpretations by Husty (1995, 1996), who used the accessible language of Bottema and Roth (1990).

Kinematic synthesis of four-bar mechanisms using kinematic mapping was discussed in Bottema and Roth (1990), originally published in 1979, and expanded upon in great detail by Ravani (1982), and Ravani and Roth (1983). In this early work, Ra-

*Address all correspondence to this author.

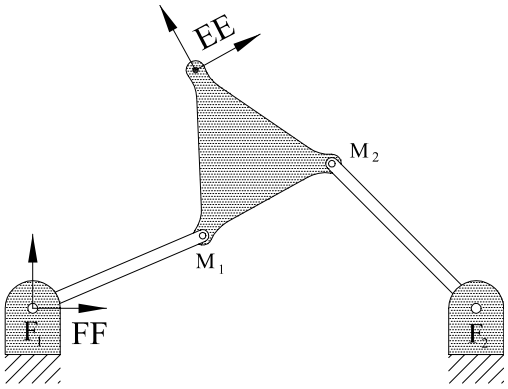

Figure 1. A FOUR-BAR LINKAGE.

vani and Roth developed the framework for performing *approximate* dimensional synthesis. While *exact* dimensional synthesis for the Burmester problem may have been implied, it has never, to our knowledge, been implemented. Results are so elegantly obtained in the kinematic mapping image space that we are compelled to expose the methodology and procedure by which these are produced.

In this image space, the kinematic constraint implied by the motion of a point bound to move upon a circle of fixed centre and radius maps to a hyperboloid of one sheet. Thus, the motion of the coupler of a planar four-bar mechanism connected with four revolute (R) pairs can be characterized by the fourth order curve of intersection of two distinct hyperboloids of one sheet in the image space.

When the kinematic constraint dictates a point moving on a line with fixed line coordinates, as with a prismatic (P) pair, the constraint surface is a hyperbolic paraboloid. Hyperboloids of one sheet and hyperbolic paraboloids are the only types of constraint surfaces associated with planar mechanisms containing only lower pair joints (Hayes and Husty, 2001). Here, we assume solutions of the five-position Burmester problem confined to four-bar mechanisms jointed with four R-pairs, not slider-cranks. Thus only image space hyperboloids of one sheet will apply.

2 Planar Kinematic Mapping

One can consider the relative displacement of two rigid-bodies in the plane as the displacement of a Cartesian reference coordinate frame EE attached to one of the bodies with respect to a Cartesian reference coordinate frame FF attached to the other. Without loss of generality, FF may be considered as fixed while EE is free to move, as is the case with the four-bar mechanism illustrated by Figure 1. Then the position of a point in EE in terms of the basis of FF can be expressed compactly as

$$\mathbf{p}' = \mathbf{R}\mathbf{p} + \mathbf{d}, \tag{1}$$

where, $\mathbf{p}$ is the 2×1 position vector of a point in EE, $\mathbf{p}'$ is the position vector of the same point in FF, $\mathbf{d}$ is the position vector of the origin of frame EE in FF, and $\mathbf{R}$ is a 2×2 proper orthogonal rotation matrix (*i.e.*, its determinant is $+1$) defined by the orientation of EE in FF indicated by ϕ.

Equation (1) can always be represented as a linear transformation by making it *homogeneous* (see McCarthy (1990), for example). Let the homogeneous coordinates of points in the fixed frame FF be the ratios $[X : Y : Z]$, and those of points in the moving frame EE be the ratios $[x : y : z]$. Then Equation (1) can be rewritten as

$$\begin{bmatrix} X \\ Y \\ Z \end{bmatrix} = \begin{bmatrix} \cos\phi & -\sin\phi & a \\ \sin\phi & \cos\phi & b \\ 0 & 0 & 1 \end{bmatrix} \begin{bmatrix} x \\ y \\ z \end{bmatrix}. \tag{2}$$

Equation (2) clearly reflects the fact that a general displacement in the plane is fully characterized by three parameters, in this case a, b, and ϕ.

2.1 Image Space Coordinates and Pole Position

The essential idea of the kinematic mapping introduced by Blashke (1911) and Grünwald (1911)is to map the three homogeneous coordinates of the pole of a planar displacement, in terms of (a, b, ϕ), to the points of a three dimensional projective image space.

The pole, P, of a planar displacement may be described in the following way. Any planar displacement that is a combination of translation and rotation may be represented by a single rotation through a finite angle about a unique fixed axis normal to the plane. Even a pure translation can be considered a rotation through an infinitesimal angle about a point at infinity on a line perpendicular to the direction of the translation. The coordinates of the piercing point of this axis with the plane of the displacement describe the pole, P. If EE and FF are initially coincident, then the coordinates of P are invariant under the its related displacement. That is, P has the same coordinates in both EE and FF. This is illustrated in Figure 2.

By using the dehomogenized form of Equation (2) one may immediately write, after setting $X_P = x_P$ and $Y_P = y_P$ and solving the resulting two simultaneous equations

$$x_P = \frac{a}{2} - \frac{b\sin\phi}{2(1-\cos\phi)}; \quad y_P = \frac{a\sin\phi}{2(1-\cos\phi)} + \frac{b}{2}.$$

The value of the homogenizing coordinate is arbitrary and may, without loss of generality, be set to $z = 2\sin\phi/2$. This means that

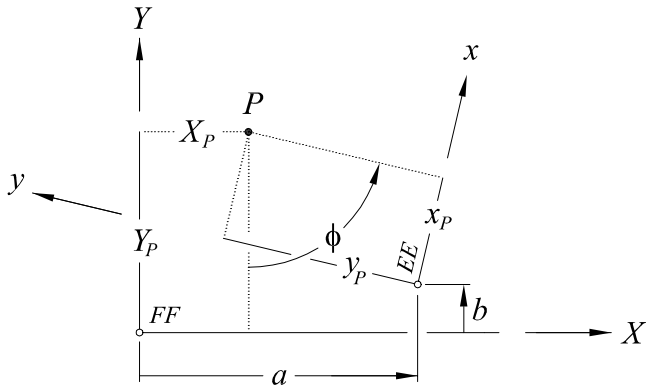

Figure 2. POLE POSITION.

both x_P and y_P must also be multiplied by this value. Then the double angle relationships

$$\sin 2\phi = 2\sin\phi\cos\phi; \quad \cos 2\phi = \cos^2\phi - \sin^2\phi$$

can be used to obtain the following homogeneous coordinates of the pole:

$$\begin{aligned} X_P = x_P &= a\sin(\phi/2) - b\cos(\phi/2) \\ Y_P = y_P &= a\cos(\phi/2) + b\sin(\phi/2) \\ Z_P = z_P &= 2\sin(\phi/2) \end{aligned} \tag{3}$$

The kinematic mapping image coordinates are defined, with respect to the pole P as follows.

$$\begin{aligned} X_1 &= a\sin(\phi/2) - b\cos(\phi/2) \\ X_2 &= a\cos(\phi/2) + b\sin(\phi/2) \\ X_3 &= 2\sin(\phi/2) \\ X_4 &= 2\cos(\phi/2). \end{aligned} \tag{4}$$

Since each distinct displacement described by (a,b,ϕ) has a corresponding unique image point, the inverse mapping can be obtained from Equation (4): for a given point of the image space, the displacement parameters are

$$\begin{aligned} \tan(\phi/2) &= X_3/X_4, \\ a &= 2(X_1X_3 + X_2X_4)/(X_3^2 + X_4^2), \\ b &= 2(X_2X_3 - X_1X_4)/(X_3^2 + X_4^2). \end{aligned} \tag{5}$$

Equations (5) give correct results when either X_3 or X_4 is zero. Caution is in order, however, because the mapping is injective, not bijective: *there is at most one pre-image for each image point*. Thus, not every point in the image space represents a displacement. It is easy to see that any image point on the real line $X_3 = X_4 = 0$ has no pre-image and therefore does not correspond to a real displacement of EE. From Equation (5), this condition renders ϕ indeterminate and places a and b on the line at infinity.

Armed with Equations (4) and (5) any displacement in terms of X_1, X_2, X_3, X_4 can be conveniently converted to the displacement of EE in terms of FF.

2.2 Representing Planar Displacements in Terms of Image Space Coordinates

By virtue of the relationships expressed in Equation (4), the transformation matrix from Equation (2) may be expressed in terms of the homogeneous coordinates of the image space. This yields a linear transformation to express a displacement of EE with respect to FF in terms of the image point:

$$\lambda \begin{bmatrix} X \\ Y \\ Z \end{bmatrix} = \begin{bmatrix} X_4^2 - X_3^2 & -2X_3X_4 & 2(X_1X_3 + X_2X_4) \\ 2X_3X_4 & X_4^2 - X_3^2 & 2(X_2X_3 - X_1X_4) \\ 0 & 0 & X_3^2 + X_4^2 \end{bmatrix} \begin{bmatrix} x \\ y \\ z \end{bmatrix}, \tag{6}$$

where λ is a proportionality constant arising from the use of homogeneous coordinates. The inverse transformation can be obtained with the inverse of the 3×3 matrix in Equation (6) as follows.

$$\mu \begin{bmatrix} x \\ y \\ z \end{bmatrix} = \begin{bmatrix} X_4^2 - X_3^2 & 2X_3X_4 & 2(X_1X_3 - X_2X_4) \\ -2X_3X_4 & X_4^2 - X_3^2 & 2(X_2X_3 + X_1X_4) \\ 0 & 0 & X_3^2 + X_4^2 \end{bmatrix} \begin{bmatrix} X \\ Y \\ Z \end{bmatrix}, \tag{7}$$

with μ being another proportionality constant. The product of these matrices is homogeneously proportional to a unit matrix:

$$\begin{bmatrix} (X_3^2 + X_4^2)^2 & 0 & 0 \\ 0 & (X_3^2 + X_4^2)^2 & 0 \\ 0 & 0 & (X_3^2 + X_4^2)^2 \end{bmatrix}.$$

Clearly, by construction in Equation (4), $X_3^2 + X_4^2 \equiv 2$.

2.3 Planar Constraint Equations

Consider the case of an R-R joint dyad. A point on EE moves on a circle on FF, whose homogeneous equation may be expressed by:

$$C_0(X^2 + Y^2) + 2C_1XZ + 2C_2YZ + C_3Z^2 = 0. \tag{8}$$

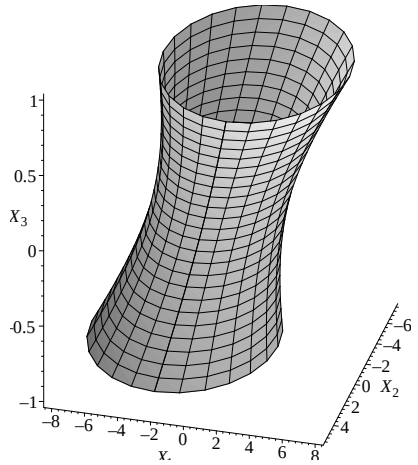

Figure 3. A HYPERBOLOID OF ONE SHEET.

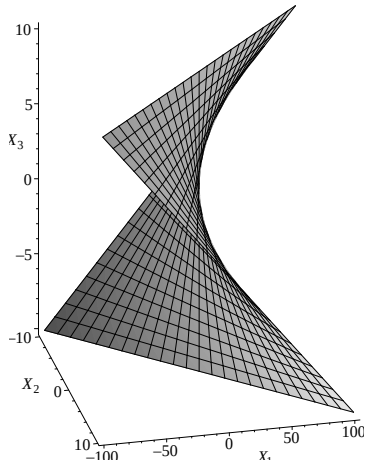

Figure 4. A HYPERBOLIC PARABOLOID.

In Equation (8) $C_0 = k$, an arbitrary constant, while $C_1 = -X_m$, $C_2 = -Y_m$, the circle centre coordinates, and $C_3 = X_m^2 + Y_m^2 - r^2$ with r being the circle radius.

Expanding Equation (6) and substituting the expressions for X, Y, and Z into Equation (8) produces a hyperboloid of one sheet in the image space, see Figure 3. The hyperboloid takes the form:

$$\begin{aligned} &C_0 z^2(X_1^2+X_2^2)+(-C_0x+C_1z)zX_1X_3 \\ &+(-C_0y+C_2z)zX_2X_3+(-C_0y-C_2z)zX_1X_4 \\ &+(C_0x+C_1z)zX_2X_4+(-C_1y+C_2x)zX_3X_4 \\ &+\frac{1}{4}[C_0(x^2+y^2)-2C_1xz-2C_2yz+C_3z^2]X_3^2 \\ &+\frac{1}{4}[C_0(x^2+y^2)+2C_1xz+2C_2yz+C_3z^2]X_4^2=0. \end{aligned} \tag{9}$$

Recall that the coordinates of a point in the moving frame EE are $(x:y:z)$. The hyperboloid is specified when a reference point $(x:y:z)$ is given together with the circle coordinates $(C_0 : C_1 : C_2 : C_3)$. The points $(X_1 : X_2 : X_3 : X_4)$ represent all possible displacements of EE relative to FF under the constraint that one point in FF moves on a circle in EE.

We can generalize the constraint hyperboloid by considering the kinematic inversion: a point on FF bound to move on a circle in EE. We thus expand Equation (5) and substitute the expressions for x, y, and z into Equation (8) and make the following simplifications. For the given circular constraint it is clear that $C_0 = 1$. We may also set $z = X_4 = 1$. The general constraint hyperboloid then becomes

$$\begin{aligned} &(X_1^2+X_2^2)+(C_1-x)X_1X_3+(C_2-y)X_2X_3 \\ &\mp(C_2+y)X_1\pm(C_1+x)X_2\pm(C_2x-C_1y)X_3 \\ &+\frac{1}{4}[(x^2+y^2)-2C_1x-2C_2y+C_3]X_3^2 \\ &+\frac{1}{4}[(x^2+y^2)+2C_1x+2C_2y+C_3]=0. \end{aligned} \tag{10}$$

When (x,y) are the coordinates of the moving point expressed in EE with $z=1$ the *upper* signs apply. If the constraint is intended to express the inverse, a point on FF bound to a circle in EE, then the *lower* signs apply *and* x, y or z is substituted wherever X, Y or Z appears. The situation of a circle moving on a point is never required in problem formulation.

However if a point is bound to a line, *i.e.*, in the case of a prismatic joint, and if one desires to treat inversions, the line may be either on FF *or* EE. Equation (10) reduces to Equation (11) if a point is bound to a line and $C_0 = 0$. This produces a hyperbolic paraboloid in the image space, see Figure 4:

$$\begin{aligned} &C_1X_1X_3+C_2X_2X_3\mp C_2X_1\pm C_1X_2\pm(C_2x-C_1y)X_3 \\ &-\frac{1}{4}[2C_1x+2C_2y-C_3]X_3^2+\frac{1}{4}[2C_1x+2C_2y+C_3]=0. \end{aligned} \tag{11}$$

The above constraint surfaces completely describe the displacements of all possible planar dyads constructed with lower pairs.

3 The Five-Position Burmester Problem

The goal of the dimensional synthesis problem for rigid body guidance of a 4R planar mechanism is to find the *moving*

circle points, M_1 and M_2 of the coupler, i.e., the revolute centres that move on fixed centred, fixed radii circles as a reference coordinate system, EE, attached to the coupler, passes through the desired poses. The *fixed centre points* for each circle are the fixed, or grounded revolute centres, F_1 and F_2, respectively. The circle and centre points are illustrated with the four-bar mechanism shown in Figure 1. For these constraints, the synthesis equations are determined using Equation (10).

What we set out to do here is to use the methods of planar kinematic mapping outlined in (Zsombor-Murray, *et al*, 2002) and set up five simultaneous constraint equations, each of which represents the image space constraint surface for a rigid body moving freely in the plane except that one point is bound to the circumference of a fixed circle. These equations are expressed in terms of the following eight variables.

i. X_1, X_2, X_3, $X_4 = 1$, the dehomogenized coordinates of the coupler pose in the image space.
ii. C_1, C_2, C_3, the coefficients of a circle equation ($C_0 = 1$).
iii. x, y, $z = 1$,the coordinates of the moving crank-pin revolute centre, on the coupler, which moves on a circle.

Since X_1, X_2, X_3 are given for five desired coupler poses, one may in principle solve for the remaining five variables (C_1, C_2, C_3, x, y) . The geometric interpretation is, five given points in space are common to, at most, four hyperboloids on one sheet. Each hyperboloid represents a 2R dyad. If two real solutions occur then all 4R mechanism design information is available (there are two circles in a feasible mechanism design result):

i. Circle centre is at $X_m = -C_1$, $Y_m = -C_2$.
ii. Circle radius is given by $r^2 = C_3 - (X_m^2 + Y_m^2)$.
iii. Coupler length is given by $L^2 = (x_2 - x_1)^2 + (y_2 - y_1)^2$.

4 Analysis

4.1 Converting Pose to Image Space Coordinates

Examine Equations (4) and divide by X_4.

$$X_1 = \frac{\left(a\tan\frac{\phi}{2} - b)\right)}{2},\ X_2 = \frac{\left(a + b\tan\frac{\phi}{2}\right)}{2},\ X_3 = \tan\frac{\phi}{2},\ X_4 = 1.$$

The five given poses being specified as (a_i, b_i, ϕ_i), $i \in \{1, ..., 5\}$, the planar coordinates of the moving point and the orientation of a line on the moving rigid body, all with respect to $(0, 0, 0^\circ)$ expressed in FF. Note that the location of the origin of FF is arbitrary, it is only shown on the fixed revolute centre in Figure 1 for convenience.

4.2 Crank Angles

If the desired five poses can be realized with a planar 4R four-bar mechanism, then at least two real solutions in

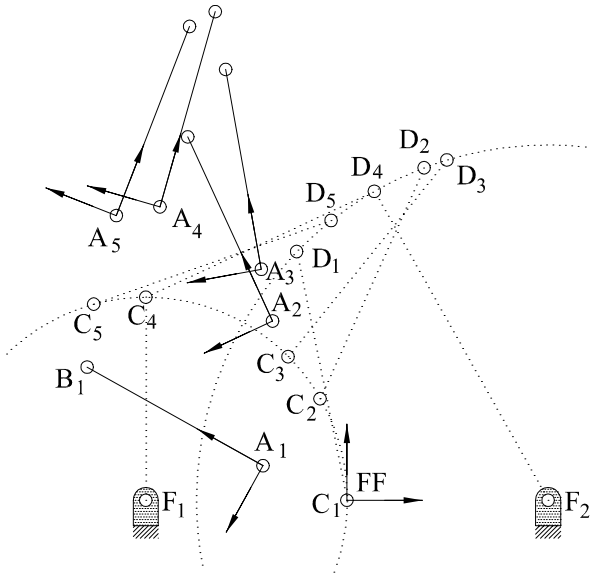

Figure 5. GENERATING THE FIVE DESIRED POSES.

(C_1, C_2, C_3, x, y) will be obtained, defining two 2R dyads sharing the coupler. To construct the mechanism in its five configurations the crank angles must be determined. To obtain the crank angles one just takes (x_1, y_1) and (x_2, y_2) and performs the linear transformation, expressed in image space coordinates, five times.

$$\begin{bmatrix} X \\ Y \\ 1 \end{bmatrix} = \begin{bmatrix} 1 - X_3^2 & -2X3 & 2(X_1X_3 + X2) \\ 2X_3 & 1 - X_3^2 & 2(X_2X_3 - X_1) \\ 0 & 0 & 1 + X_3^2 \end{bmatrix} \begin{bmatrix} x \\ y \\ 1 \end{bmatrix}.$$

(X, Y) come in five pairs because five poses are specified. These are the Cartesian coordinates of the moving revolute centres expressed in FF, and implicitly define the crank angles. For a practical design one must check that the solution did not separate crank pin coordinates in unconnected mechanism branches.

4.3 Pose Constraint Equation

Given the constraints imposed by four revolute joints, the pose constraint equation (synthesis equation) is given by Equation (10) with the upper signs used. For each of the five poses we obtain:

$$\begin{aligned} &(X_1^2 + X_2^2) + (C_1 - x)X_1X_3 + (C_2 - y)X_2X_3 \\ &-(C_2 + y)X_1 + (C_1 + x)X_2 + (C_2x - C_1y)X_3 \\ &+\tfrac{1}{4}[(x^2 + y^2) - 2C_1x - 2C_2y + C_3]X_3^2 \\ &+\tfrac{1}{4}[(x^2 + y^2) + 2C_1x + 2C_2y + C_3] = 0. \end{aligned} \tag{12}$$

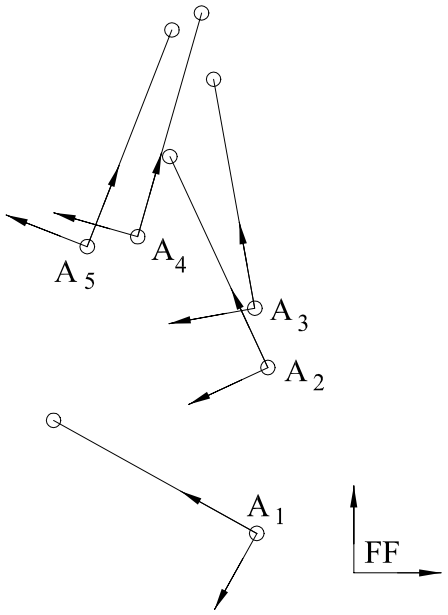

Figure 6. THE FIVE DESIRED POSES.

Parameter	Value
F_1	(-8,0)
F_2	(8,0)
F_1F_2	16
F_1C	8
CD	10
DF_2	14

Table 1. THE GENERATING MECHANISM

i^{th} Pose, A_i	a	b	φ (deg)
1	-3.339	1.360	150.94
2	-2.975	7.063	114.94
3	-3.405	9.102	100.22
4	-7.435	11.561	74.07
5	-9.171	11.219	68.65

Table 2. FIVE RIGID BODY POSES IN FF.

5 Example and Verification

The kinematic mapping solution to the five-position Burmester problem is illustrated with the following example problem. In order to verify our synthesis results, we started with Figure 5, wherein one sees a four-bar mechanism design represented by dotted crank pin circles and a coupler CD which has been placed in five feasible poses. Then an arbitrary point A and orientation line AB were specified. These were used to specify the given five poses, listed in Table 2. The fixed revolute centres and link lengths of the four-bar mechanism used to generate the poses, which we can check for verification, are listed in Table 1, all coordinates given relative to FF. The coordinate information obtained from these were inserted into the five synthesis equations. The results at the end constitute obvious confirmation concerning the effectiveness of the kinematic mapping approach to solving the Burmester problem.

Given the Cartesian coordinates of five positions of a reference point on a rigid body, together with five orientations of the rigid body which correspond to the positions, all relative to an arbitrary fixed reference frame, FF. The reference point is the origin of a coordinate system, A, attached to the rigid body. In Figure 6 the five poses are indicated by the position of A and the orientation of a line in the direction x_A axis. The coordinates and orientations are listed in Table 2.

The given five poses are mapped to five sets of coordinates in the image space. Using a computer algebra software package, we substitute the corresponding values for X_1, X_2, X_3, together with $X_4 = 1$ into Equation (12) yields the following five quadratics in C_1, C_2, C_3, x, and y:

$$\begin{aligned} &51.62713350 - 26.52347891C_1 + 28.43187273x \\ &+3.439909575y + 10.80321393C_2 + 3.971769828y^2 \\ &+3.971769828x^2 - 6.943539655C_1x + 3.971769828C_3 - \\ &6.943539655C_2y - 3.858377808C_1y + 3.858377808C_2x = 0 \end{aligned} \quad (13)$$

$$\begin{aligned} &50.78111719 - 5.144112496C_1 + 13.24300208x \\ &-.485305000y + 12.21272826C_2 + .8645567222y^2 \\ &+.8645567222x^2 - .7291134440C_1x + .8645567222C_3 \\ &-.7291134440C_2y - 1.567873365C_1y + 1.567873365C_2x = 0 \end{aligned} \quad (14)$$

$$\begin{aligned} &57.40558942 - 4.139456673C_1 + 11.62418825x \\ &+2.110482435y + 11.06529652C_2 + .6078497318y^2 \\ &+.6078497318x^2 - .2156994635C_1x + .6078497318C_3 \\ &-.2156994635C_2y - 1.196410852C_1y + 1.196410852C_2x = 0 \end{aligned} \quad (15)$$

$$\begin{aligned} &74.12376162 - 5.833830775C_1 + 7.121746695x \\ &+8.099525062y + 9.071273378C_2 + .3923221773y^2 \\ &+.3923221773x^2 + .2153556452C_1x + .3923221773C_3 \\ &+.2153556452C_2y - .7545122328C_1y + .7545122328C_2x = \end{aligned} \quad (16)$$

$$\begin{aligned} &76.96602922 - 6.723290851C_1 + 5.212549019x \\ &+9.256210937y + 8.224686519C_2 + .3665516768y^2 \\ &+.3665516768x^2 + .2668966465C_1x + .3665516768C_3 \\ &+.2668966465C_2y - .6827933120C_1y + .6827933120C_2x = 0 \end{aligned} \quad (17)$$

Solving the system of Equations (13)-(17) yields four sets of values for C_1, C_2, C_3, x, and y, two being real, and the remaining two being complex conjugates. The two real sets of hyperboloid coefficients are listed in Table 3. The corresponding synthesized four-bar fixed revolute centres and link lengths are listed in Table 4, rounded to same three decimal places as the graphically determined generating mechanism listed in Table 1.

Coefficient	Solution 1	Solution 2
C_1	-7.983138944	7.997107716
C_2	-.027859304	-.000953257
C_3	-131.4773813	-.022545268
x	2.932070052	-3.579426217
y	-8.023883728	-.435620093

Table 3. THE HYPEBOLOID COEFFICIENTS

Parameter	Value
F_1	(-7.997,0.001)
F_2	(7.983,-0.023)
F_1F_2	15.980
F_1C	7.999
CD	10.003
DF_2	13.972

Table 4. THE SYNTHESIZED MECHANISM

While the synthesized mechanism link lengths and centre coordinates are affected by the numerical resolution of the graphical construction of the generating mechanism, we believe this example demonstrates the utility of kinematic mapping to solving the five-position Burmester problem.

6 Computational Pathology

Notice that feasible slider-crank solutions were implicitly excluded by choosing to set $C_0 = z = 1$ rather than, say, $C_2 = y = 1$. This is similar to excluding half-turn EE orientations by setting $X_4 = 1$ rather than, say, $X_3 = 1$. It is recommended that algorithmic implementation should retain $X_4 = 2\cos(\phi/2)$ and contain features to replace $C_0 = 1$ with C_1, C_2 or $C_3 = 1$ and $z = 1$ with x or $y = 1$ should results where $x \to y \to \infty$ with $C_0 = z = 1$ occur.

7 Conclusions

We have used kinematic mapping to solve the five position planar Burmester problem. Five rigid body poses are mapped to points in a three dimensional projective image space and are used directly as inputs to generate five quadratic constraint surface equations in that space. The solutions, when they exist, give the coefficients of the hyperboloids having the five points in common. Each hyperboloid yields a fixed revolute centre, link lengths, crank angles, and coupler attachment points. This method is elegant in that the design task for any composition of R and P joints (open RR, PR, and RP chains) can be treated with a single formulation with no special cases.

REFERENCES

1. Blaschke, W., 1911, "Euklidische Kinematik und nichteuklidische Geometrie", *Zeitschr. Math. Phys.*, Vol. 60, pp. 61-91 and 203-204.
2. Bottema, O. & Roth, B., 1990, *Theoretical Kinematics*, Dover, ch.XI, pp.393-445.
3. Burmester, L., 1888, *Lehrbuch der Kinematik*, A. Felix, Leipzig.
4. Ching Yu Chang, Angeles, J., González-Palacios, M., 1991, "A Semi-graphical Method for the Solution of the Burmester Problem", *ASME Adv. in Des. Auto.*, DE-Vol. 32-2, pp 321-326.
5. Grünwald, J., 1911, "Ein Abbildungsprinzip, welches die ebene Geometrie und Kinematik mit der räumlichen Geometrie verknüpft", *Sitzber. Ak. Wiss. Wien*, Vol. 120, pp. 677-741.
6. De Sa, S., Roth, B., 1981, "Kinematic Mappings. Part 1: Classification of Algebraic Motions in the Plane", *ASME, J. of Mech. Design*, Vol. 103, pp. 585-591.
7. Hayes, M.J.D., Husty, M.L., 2001, "On the Kinematic Constraint Surfaces of General Three-Legged Planar Robot Platforms", submitted to *Mechanism and Machine Theory*.
8. Husty, M.L., 1995, "Kinematic Mapping of Planar Tree(*sic.*)-Legged Platforms, *Proc. of 15th Cdn. Conf. of Appl. Mech.*, Victoria, v.2, ISBN 0920049-06, pp. 876-877.
9. Husty, M.L., 1996, "An Algorithm for Solving the Direct Kinematics of General Stewart-Gough Platforms", *Mechanism and Machine Theory*, Vol. 31, No. 4, pp. 365-379.
10. McCarthy, J.M., 1990, *An Introduction to Theoretical Kinematics*, The M.I.T. Press, Cambridge, Mass., U.S.A..
11. McCarthy, J.M., 2000, *Geometric Design of Linkages*, Springer, New York, NY., U.S.A..

12. Murray, A.P., McCarthy, J.M., August 1996, *Constraint Manifold Synthesis of Planar Linkages*, Proceedings of ASME DETC: Mechanisms Conference, Irvine CA.
13. Ravani, B., 1982, *Kinematic Mappings as Applied to Motion Approximation and Mechanism Synthesis*, Ph.D. Dissertation, Stanford University, Stanford, Ca., U.S.A..
14. Ravani, B., Roth, B., 1983, "Motion Synthesis Using Kinematic Mappings", ASME, *J. of Mechanisms, Transmissions, & Automation in Design*, Vol. 105, pp. 460-467.
15. Zsombor-Murray, P.J., Chen, C. & Hayes M.J.D., 2002, "Direct Kinematic Mapping for General Planar Parallel Manipulators", to appear in *Proc. CSME Forum*, Kingston, ON, Canada.